

Direct evidence for 8-interstitial-controlled nucleation of extended defects in c-Si

F. Schiettekatte,^{a)} S. Roorda, R. Poirier, M. O. Fortin, S. Chazal, and R. Héliou

Groupe de Recherche en Science et Technologie des Couches Minces et Département de Physique, Université de Montréal, Montréal, Québec, Canada, H3C 3J7

(Received 11 May 2000; accepted for publication 1 November 2000)

The areal density of extended defects in P-implanted and annealed Si is observed to increase with ion dose to the power 8. A simple model based on Poisson statistics applied to point defects created during ion implantation shows that such a dependence corresponds to enhanced stability of interstitial clusters consisting of at least eight interstitial atoms, and it implies an interstitial “clustering” radius of 0.8 nm. The direct observation of “ $n=8$ ” confirms the curious behavior observed earlier in transient-enhanced diffusion of B in Si, and provides a quantitative explanation of the threshold dose for the formation of extended defects in ion-implanted Si. © 2000 American Institute of Physics. [S0003-6951(01)03001-7]

Complete understanding and detailed modeling of the removal of ion-implantation damage in Si and the accompanying transient-enhanced impurity diffusion (TED) are hampered by a lack of insight into the clustering phase in the defect evolution. The ion-implantation process itself produces large numbers of vacancies (V) and interstitials (I) and their immediate complexes after association with an impurity atom. Many years of mostly spectroscopic studies^{1,2} have elucidated the structure and properties of many of those defects. Since the implantation injects new atoms into the crystal, the number of I no longer balances the V . The end result of the defect annealing leads often to the formation of extended defects such as the $\{311\}$ defect and, subsequently, to even larger structures such as dislocation loops, which actually contain the excess I (+1 model).³ These “large” structures have been well characterized, even quantitatively, by transmission electron microscopy (TEM).⁴ The transition region in between, where defect clusters are made up of 3–300 individual point defects, however, remains elusive to the point where it has been described as “the missing link.”^{5,6}

Significant progress has been made recently, both experimentally and theoretically. Deep-level transient spectroscopy analysis can now distinguish between I clusters and $\{311\}$ -type defects.^{5,7} Photoluminescence results have been interpreted to mean that a $\{311\}$ is structurally different from an I cluster, and not just a larger version of it.⁸ Detailed tight-binding and *ab initio* calculations show that the formation energy per I is decreasing with cluster size,⁹ but these calculations did not show enhanced stability of “ $n=8$ ” clusters. Other calculations, however, did show significantly lower formation energies for $n=4$ and $n=8$ clusters than for clusters only 1 atom larger or smaller.¹⁰ Such an enhanced stability had been deduced from inverse modeling of the I cluster ripening process and its effect on broadening (TED) of B markers in Si.¹¹ In this letter, we augment these recent

results with a direct observation of “ $n=8$ ” enhanced stability.

Undoped n -type Czochralski-grown Si wafers ($\rho \geq 10 \Omega \text{ cm}$, 300 μm thick) were implanted at 7° off normal with 230 keV P ions at wafer temperatures of 23 ± 1 , 150 ± 3 , and 300 ± 2 °C. The wafers were then annealed in a rapid thermal annealing (RTA) system at 1000 °C for 30 s under N_2 atmosphere. The density, size, and configuration of the extended defects in higher-dose samples were determined by plan-view transmission electron microscopy (pv-TEM). Reliably extracting a power-law dependence of the extended defect density on ion dose requires that the former be measured over several orders of magnitude, and most data points fall well below the threshold for observation by TEM. Therefore, the extended defects in lower-dose samples were delineated using a Wright etch solution¹² and observed by optical microscopy. A Wright etch delineates a defect as a result of an increased oxidation rate in the defect area. In order to produce an optically visible pit, the defect has to be large enough and must involve several thousands of atoms (i.e., extended defect). Also, a fairly good correspondence is found in the literature between the position of the extended defects and the etch pits.¹³ Hence, small defect clusters should not produce such visible etch pits, besides the fact that they are not expected to survive the thermal anneal preceding the Wright etch. The samples were etched $\sim 2 \mu\text{m}$, well below the region where the extended defects are located, near $R_p \sim 0.5 \mu\text{m}$.

Although not shown here, the as-implanted and (higher-dose) annealed samples were also evaluated by channeling and TEM and the results¹⁴ confirmed that the samples obey the “+1” model for the room-temperature (RT) implantations, but a modified “+1” model for the hot implants.

Figure 1 shows how the extended defect density depends on dose for different implant temperatures, as measured by TEM (solid symbols) and Wright etch (open data points). It can be divided in two parts. For higher doses, the extended defect density stabilizes close to a linear increase and is much lower for the 300 °C implants, but these extended defects are significantly larger than those induced by RT

^{a)}Author to whom correspondence should be addressed; electronic mail: francois.schiettekatte@umontreal.ca

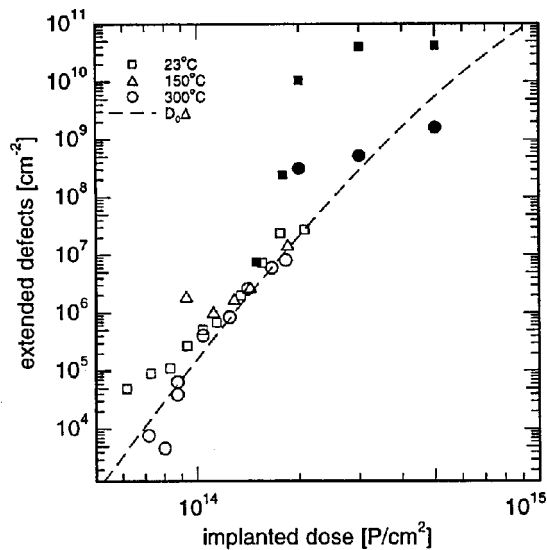


FIG. 1. Extended defect densities in annealed samples measured by TEM (filled symbols) and revealed by Wright etch solution (open symbols) as a function of dose ϕ .

implantation.¹⁴ However, in this letter we will be mainly concerned with the lower-dose regime. There, we observe a remarkably steep increase of the number of extended defects with dose (5–6 orders of magnitude for doses between 0.6×10^{14} and 2×10^{14} P/cm²). In this part (below 1.7×10^{14} P/cm²), no noticeable difference is observed in the extended defect areal density between room-temperature and 300 °C implants.

To understand the process responsible for such a steep increase, we propose an analysis of the data in terms of the statistical distribution of the implantation damage. Here, we made the following assumptions: (i) During the implantation, the point defects are generated evenly over the implantation depth d , as schematically depicted in Fig. 2. (ii) All the point defects (I and V) included inside a subvolume γ recombine with each other, leading to an excess of only one type of defect within γ at the end of the implantation. The point defects have, even at low temperature, some mobility during the ion implantation and, therefore, it is reasonable to assume that within each sufficiently small subvolume γ , all I recombine with the available V until only one type of point defect remains. (iii) The remaining defects are considered to form a cluster. (γ can thus be thought of as a “clustering” volume.)

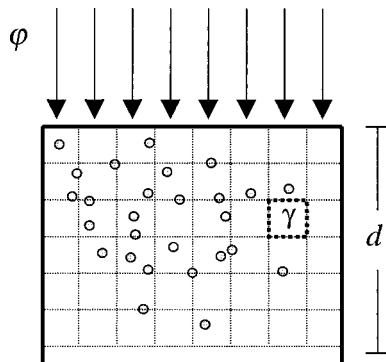


FIG. 2. Schematic cross-sectional representation of the point-defect distribution in implanted silicon over the implanted depth d . A subvolume γ , for which the probability $Q_{n \geq n_0}$ is calculated [Eq. (3)], is also shown.

Single-collision cascade defect-cluster formation¹⁵ or defect-induced nucleation of amorphous zones¹⁶ are not considered.

Since N ions are implanted over an area Σ and a depth d of the sample (dose $\phi = N/\Sigma$), the average volume density of point defects will be $\phi = kN/\Sigma d$. Here, k represents the number of stable point defects per incident ion. Because of the first assumption, the probability to find m point defects of each type (I or V) within γ will follow Poisson’s law

$$P_m(\lambda) = e^{-\lambda} \lambda^m / m!, \quad \lambda = \gamma \phi. \tag{1}$$

Consequently, considering the second and third assumptions, the probability to form an excess of n point defects of one type within γ , and thus to find a cluster consisting of n point defects is

$$Q_n(\lambda) = \sum_{m=0}^{\infty} P_{n+m}(\lambda) P_m(\lambda). \tag{2}$$

This statistic describes the end result of the point-defect accumulation–recombination process, which happens continuously during the implantation. Then, as a result of the implantation process, the probability that, within γ , a cluster consisting of n_0 or more point defects (i.e., $n \geq n_0$) occurs is given by

$$Q_{n \geq n_0}(\lambda) = \sum_{n=n_0}^{\infty} Q_n(\lambda). \tag{3a}$$

It can be shown that, for small values of λ (i.e., low doses),

$$Q_{n \geq n_0}(\lambda) \approx \frac{\lambda^{n_0}}{n_0!} \propto \phi^{n_0}. \tag{3b}$$

The areal density of such clusters will be given by

$$\Delta = \frac{d}{\gamma} Q_{n \geq n_0}(\lambda). \tag{4}$$

The probability to form clusters at least of n_0 point defects scales as a power n_0 of the dose after a low-dose implantation. At this point, both I and V clusters are considered to be present inside the sample, with an excess of I clusters.

Then, during the initial stages of a subsequent thermal anneal, energetically weak clusters will disassemble, and the resulting interstitials will recombine with other defects [it is known that the V disappear quickly ($\ll 1$ s) (Ref. 17) during the first stages of an annealing because of the excess of I] or diffuse away to deeper layers or to the surface. Clearly, clusters that decompose at lower temperatures do not contribute to nucleation of extended defects.

The situation is different for somewhat larger, stable clusters that disassemble only at higher temperature, a temperature where the crystal mobility allows extended defect nucleation to proceed. If we consider that only clusters larger than a certain number n_0 of interstitials are stable enough to survive until extended defects nucleate, then the defect density must depend on the number of available stable clusters. The low-dose approximation of Eq. (3) fitted to the data of Fig. 1 reveals an augmentation following $\phi^{8.1 \pm 0.7}$ at lower doses. This indicates that only the clusters consisting of $n \geq 8$ are actually stable enough to survive the first annealing stages and participate to the extended defect nucleation process.

The model only considers defects evenly distributed over the implantation depth d . This is not actually the case, neither is it at the local scale. However, such disparities only affect the numerical value of γ . The exponent n_0 , which is the main feature of the model, is relatively insensitive to such complications. For any defect distribution function that includes a density of defects increasing linearly with dose (at least in first order), the probability to find n defects in the same region will be the n product of the probabilities, which will always scale as φ^n , until second-order terms become dominant (e.g., amorphization). The value of $n_0=8$ should thus reflect a fundamental effect.

The direct observation of an exponent 8, indicative of enhanced stability of $n=8$ interstitial clusters is in interesting agreement with the results of Cowern *et al.*,¹¹ who estimated the formation energy of n -interstitial clusters as a function of n by an inverse modeling of the TED of B in Si. They found a clear decrease in energy for this exact value of $n=8$, and $n \geq 12$, which supports very well our argument concerning the higher stability of such clusters.

Some conclusions can also be drawn from the other parameters of Eq. (4). A function of the form $D_0 \Delta$, with $n_0=8$, $d=550$ nm, and $k=100$, has been fitted to the extended defect areal density data obtained for the 300 °C implant. The best fit, represented as a dashed line in Fig. 1, gives $\gamma=2 \pm 1$ nm³ and $D_0=10^{-2.8 \pm 1.7}$. A tight correlation between γ and D_0 is responsible for the large uncertainty on their value. Nevertheless, a “clustering” radius can be extracted from γ by assuming that this volume represents a sphere of radius r_c (i.e., $\gamma=4\pi r_c^3/3$), which gives $r_c=0.8 \pm 0.15$ nm. This value is similar to the trap limited I diffusion length for 20 min at room temperature, according to the diffusion coefficient assumed by Jaraíz *et al.*¹⁷ (our implantation times ranged from 5 to 15 min). The value of $D_0 \sim 10^{-3}$ suggests that 10^3 clusters are involved in the nucleation of each extended defect in this case.

The extended defects have been shown to occur when the areal density of point defects after implantation reaches a certain level (the “Schreutelkamp criterion”¹⁸). However, this criterion does not apply to implantation above RT. The number of point defects after implantation at 150 and 300 °C is much smaller than for RT implantation and, within the relevant dose range, independent of ion dose,¹⁴ whereas the threshold ion dose for extended defect formation is relatively insensitive to the implantation temperature (see Fig. 1). The present model allows a generalization of the threshold dose to other implantation temperatures. At RT, the number of n clusters increases at the same rate φ^n for every cluster size n since they are all stable. Above RT, $I-V$ recombination may reduce drastically the number of small clusters without af-

fecting significantly the larger ones. A more reliable (but not as easily measurable) criterion for extended defect formation would then be the number of large $n \geq n_0$ clusters.

The failure of the +1 model for low doses is a natural consequence of the Poisson statistics explored in this work. The total number of interstitial atoms retained depends on the number of stable clusters. Since only small clusters are formed at low doses, the I contained in these defects are lost during the first stages of a thermal anneal.

In conclusion, these experiments show that at low doses the density of extended defects in implanted Si increases as a power of 8 of the dose. A probabilistic interpretation of these results indicates clearly that this is a result of the enhanced stability of the eight interstitials. Our results also suggest that deviations from the Schreutelkamp criterion and the “+1” model for above-RT implantation is due to the higher decomposition rates of small clusters compared to larger ones during such implantation.

The authors are grateful to Pierre Bérichon, Réal Gosselin, Laurent Isnard, and Martin Chicoine for their technical assistance, and to Jim Sethna (Cornell University) for fruitful discussions. This work benefitted from grants from the NSERC of Canada and FCAR of Quebec.

- ¹S. T. Pantelides, *Deep Centers in Semiconductors* (Gordon and Breach, New York, 1986).
- ²J. Mayer, L. Erikson, and J. A. Davies, *Ion Implantation in Semiconductors* (Academic, New York, 1970).
- ³M. D. Giles, *J. Electrochem. Soc.* **138**, 1160 (1991).
- ⁴J. Li and K. S. Jones, *Appl. Phys. Lett.* **73**, 3748 (1998).
- ⁵J. L. Benton, S. Libertino, P. Kringhøj, D. J. Eaglesham, J. M. Poate, and S. Coffa, *J. Appl. Phys.* **82**, 120 (1997).
- ⁶Y. H. Lee, *Appl. Phys. Lett.* **73**, 1119 (1998).
- ⁷S. Libertino, J. L. Benton, S. Coffa, and D. J. Eaglesham, *Mater. Res. Soc. Symp. Proc.* **504**, 3 (1999).
- ⁸S. Coffa, S. Libertino, and C. Spinella, *Appl. Phys. Lett.* **76**, 321 (2000).
- ⁹J. Kim, F. Kirchhoff, J. W. Wilkins, and F. S. Khan, *Phys. Rev. Lett.* **84**, 503 (2000).
- ¹⁰M. M. De Souza, M. P. Chichkine, and E. M. Sankara Narayanan, *Mater. Res. Soc. Symp. Proc.* **610**, B11.3.1 (2000).
- ¹¹N. E. B. Cowern, G. Mannino, P. A. Stolk, F. Roozeboom, H. G. A. Huizing, J. G. M. van Berkum, F. Cristiano, A. Claverie, and M. Jaraíz, *Phys. Rev. Lett.* **82**, 4460 (1999).
- ¹²M. Wright Jenkins, *J. Electrochem. Soc.* **124**, 757 (1977).
- ¹³D. J. Stirland, *Appl. Phys. Lett.* **53**, 2432 (1988).
- ¹⁴F. Schiettekatte, S. Roorda, R. Poirier, M. O. Fortin, S. Chazal, and R. Héliou, *Nucl. Instrum. Methods Phys. Res. B* **164-165**, 425 (2000).
- ¹⁵M. J. Caturla, T. D. de la Rubia, and G. H. Gilmer, *Nucl. Instrum. Methods Phys. Res. B* **106**, 1 (1995).
- ¹⁶L. J. Lewis and R. M. Nieminen, *Phys. Rev. B* **54**, 1459 (1996).
- ¹⁷M. Jaraíz, G. H. Gilmer, J. M. Poate, and T. D. de la Rubia, *Appl. Phys. Lett.* **68**, 409 (1996).
- ¹⁸R. J. Schreutelkamp, J. S. Custer, J. R. Liefing, W. X. Lu, and F. W. Saris, *Mater. Sci. Rep.* **6**, 275 (1991).